Switching Colloidal Superstructures by Critical Casimir Forces

Nguyen, T.A.; Newton, A.; Veen, S.J.; Kraft, D.J.; Bolhuis, P.G.; Schall, P.

DOI
10.1002/adma.201700819

Publication date
2017

Document Version
Other version

Published in
Advanced materials

ADVANCED MATERIALS

Supporting Information

for *Adv. Mater.*, DOI: 10.1002/adma.201700819

Switching Colloidal Superstructures by Critical Casimir Forces

*Truc A. Nguyen, Arthur Newton, Sandra J. Veen, Daniela J. Kraft, Peter G. Bolhuis, and Peter Schall**

Supporting Information for article

Switching Colloidal Superstructures by critical Casimir forces

Truc A. Nguyen, Arthur Newton, Sandra J. Veen, Daniela J. Kraft, Peter G. Bolhuis and Peter Schall[*]

In this document, we provide details about the particle synthesis and experimental procedures, the particle pair potential and simulation model. We also report on trimer particle chains that exhibit a similar collapse transition as the dimer particles presented in the main manuscript.

Particle synthesis. As explained in the manuscript, the dimer particles are composed of sterically stabilized PMMA spheres with a fluorescently labelled NBD-MAEM core and non-fluorescent shell. The PMMA spheres were synthesized using dispersion polymerization with steric stabilization provided by poly(12-hydroxystearic acid) grafted copolymer (PHS-g-PMMA) following Elsesser *et al.* [1]. Colloidal clusters were fabricated by encapsulating the spherical PMMA particles in toluene droplets in an aqueous phase and selectively evaporating the toluene [2]. To obtain patchy particles, we swell a 0.8%w/w aqueous dispersion of clusters in the presence of 0.1%w/w sodium dodecyl sulfate with a 10%v/v monomer mixture consisting of 97:2:1 w/w methylmethacrylate : methacrylic acid : ethylene glycol dimethacrylate. We polymerize the swollen particles in an oil bath at 80°C by addition of aqueous potassium persulfate (final concentration in solution: 1.67 mM). The potassium persulfate imparts sulfate charges to the PMMA shell, rendering it hydrophilic with a low surface charge density. The surface of the patch not encapsulated by the PMMA shell is equivalent to that of the PMMA spheres. Therefore, the patches are sterically stabilized by PHS-g-PMMA making them hydrophobic. To separate a synthesized batch into pure dimer,

trimer, and higher-symmetry particles, we employ density gradient centrifugation using a sucrose gradient in water. By extracting the 2nd and 3rd band using a syringe, we obtain a high purity of dimer and trimer particles, respectively. The particles are subsequently suspended in the binary liquid of heavy water and 3-methyl-pyridine (3MP).

Experiments. To exploit specific interactions of the patches and shells, we prepared binary mixtures with compositions on both sides of the critical point, a 3MP-poor solvent with 3MP weight fraction $c_{3MP} = 0.25$, smaller than that of the critical composition, $c_c = 0.28$ [3], and a 3MP-rich solvent with 3MP weight fraction $c_{3MP} = 0.31 > c_c$. Previous studies have shown that strong critical Casimir interactions arise between the surfaces that have affinity for the minority phase of the binary solvent. As in previous studies, we work at temperatures below the phase separation temperature where the two solvent components 3MP and water form a homogenous mixture. By preparing two different solvent compositions, left and right of the critical point, we induce selective attractive critical Casimir interactions between the hydrophobic or the hydrophilic parts of the particles. The final suspensions are prepared at a colloid volume fraction of 0.2% and filled into glass capillaries, which are subsequently flame sealed to prevent compositional changes associated with evaporation.

To induce critical Casimir interactions, we heat the suspension to temperatures $\Delta T = T - T_c$ below the critical temperature $T_c = 38.55$ °C. To keep equilibration times short, we always first equilibrated the suspension at $\Delta T = 5$ °C, where critical Casimir interactions are still negligible and the particles remain suspended. We then raised the temperature to the final desired value close to T_c.

We follow the assembly of particles directly in real space by imaging individual particles in an area of 104 μm by 104 μm using confocal microscopy. From the images, we determine the positions of the fluorescently labelled spherical ends with an accuracy of ~0.02

μm in both directions of the imaged plane. For each measurement, a series of at least 3000 images was recorded to ensure sufficient statistics. To always start from a dispersed sample, we first equilibrated the system at $\Delta T = 5\,°C$ for at least 15 minutes before heating the sample to the final temperature.

Particles with smaller patches

We also explored the role of the patch width. To obtain particles with smaller patches, we added increasingly thick PMMA shells around the colloidal clusters, resulting in decreasing patch-to-shell aspect ratios. To do so we used larger amounts of methylmethacrylate (MM) during the swelling process. Specifically, we used two and four times the amount as used for the particles in the main manuscript. We found that the resulting particles have significantly thicker shells as seen in the SEM image in **Figure S2**, inset. Remarkably, we observe that as a result of the smaller patch width, the assembled structures become more distinct and directed, while the assembly is still fully reversible. A typical assembled dimer-particle structure obtained with four times the amount of MM during synthesis is shown in Figure S2. Only

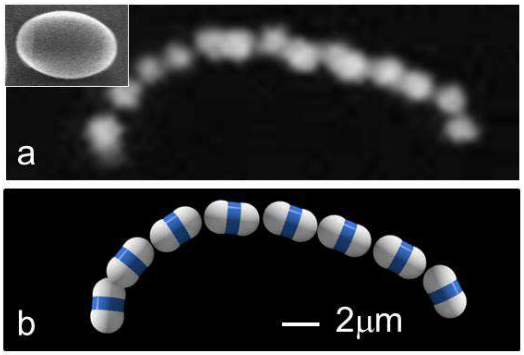

Fig. S1 Directed bonding of small-patch particles

Confocal microscope image (a) and schematic (b) of long chains assembled from small-patch dimer particles. Inset in (a) shows an SEM image of a dimer particle, exhibiting a much thicker shell than the particles used in the main manuscript. Decreasing the patch-to-shell aspect ratio narrows the available surface region to bind, resulting in very distinct, directed structures.

single bonding is observed, resulting in a long directed chain. We also found that further tuning of the specific bonding topology is possible by varying the amount of added salt that screens the electrostatic repulsion of the particles. These results ultimately open the door to precise engineering of bonding geometries.

Potential optimization. Previous work has demonstrated that the aggregation behaviour of spherical colloids in (near) critical fluids can be modelled via a superposition of critical Casimir attraction and electrostatic repulsion [4,5]. We extend this model to dumbbells by modelling the particles as two touching fused hard spheres with radius R as explained in the main text. The interaction potential is therefore defined by ξ_0 and critical Casimir amplitude A_{Cas}, which are the only free parameters. To find these parameters, we compare the experimental and simulated radial distribution functions (rdf) based on the centres of mass of each of the dumbbell spheres. However, the standard definition of the rdf is overwhelmed by the presence of the 'trivial neighbour', the sphere that is directly attached to any specific dumbbell sphere, thus rendering it insensitive to changes in the potential. Instead, we make use of the minimum distance $g_{md}(r)$, a radial distribution function that ignores the trivial neighbour, and takes only into account the sphere nearest to the sphere under consideration other than the trivial one.

As we cannot simply invert the $g_{md}(r)$ into a pair potential, we perform many Monte Carlo simulations with a predefined set of temperature-dependent potentials and subsequently find which potential best reproduces the experimentally obtained $g_{md}(r)$.[6] We globally fitted the experimental $g_{md}(r)$ across the entire temperature range using the above-mentioned scaling of the correlation length. We quantify the degree of similarity of the experimental and simulated $g_{md}(r)$ using the Jensen-Shannon divergence. To account for experimental inaccuracies and particle polydispersity, we convoluted the distributions obtained from simulation with a Gaussian of width w, and compared the broadened distributions with the experimental results.

We find that the smallest Jensen-Shannon divergence is obtained for ξ_0=1.6nm and $w = 0.09$. Latter value is very reasonable considering that the particle polydispersity is around 5%, and the in-plane and out-of-plane tracking inaccuracies are around 1 and 3% of the particle size, respectively. The resulting potentials are shown in Fig. 2a of the manuscript.

Simulations. For the Monte Carlo simulations, we placed $N = 100$ dumbbell particles in a cubic box of size $L = 64\,R$ and applied periodic boundaries in the *x*-*y* direction. The number of particles was chosen to correspond roughly to the experimentally observed number of dumbbells. The solvent is taken into account implicitly; the Monte Carlo moves have an intrinsic step size that sets the effective diffusion constant. In order to minimize hysteresis effects during aggregation we employed an annealing procedure. Starting far from T_C at $\Delta T = 1.6$K where the attraction is small, we performed 10^6 equilibration and 10^6 production cycles, where a cycle consists of moving each particle (translating and/or rotating) once on average, before increasing the temperature by 0.05K. This procedure was repeated until $\Delta T = 0.85$K corresponding to a strong Casmir interaction. By performing this scheme for several values of ξ_0, we found that $\xi_0 = 1.6$nm fits the experimentally observed $g_{md}(r)$ best. More details of the simulations can be found in [6].

Collapse of network structure. To model the collapse of the chain-like network structure, a non-equilibrium network-like structure needs to be generated. We do this by using a diffusion-limited aggregation (DLA) scheme, where we only perform cluster moves [7], which are always accepted (as long as there is no hard core overlap). A cluster is defined as a set of contiguous particles, where we consider two dumbbells to be contiguous when any two spheres of the dumbbell are closer than $0.16\,R$. This procedure quickly results in a network-like structure in which the particles have not been allowed to equilibrate due to the exclusive use of cluster moves. This network structure is quenched into a local energy minimum via

single particle MC moves with very small translation and rotation step sizes ($\delta_t = 0.01\sigma, \delta_r = 0.03$ rad), employing a sufficiently strong and short-ranged Casimir attraction ($\Delta T = 0.5K$) so that the system becomes trapped in this network like structure. This procedure is repeated until five initial structures are generated. These initial configurations are relaxed via single particle translation and rotation MC moves with small step sizes ($\delta_t = 0.01\sigma, \delta_r = 0.03$ rad for 10^7 MC cycles, where every MC cycle has N_{part} translation and rotation moves. This roughly corresponds to a relaxation of several minutes [8]. The resulting relaxation of the total energy versus time shows that a short-ranged attraction obtained far from T_C cannot equilibrate this structure to a more compact structure, because the dumbbells only feel their local neighbourhood, which is already minimized in the quenching step. However, for longer-ranged interactions very close to T_C (where the correlation length diverges) indeed a full collapse of the structure occurs, lowering the energy of the system significantly. From the snapshots at $\Delta T = 0.01$K shown in Fig. 5b, it follows that the network chain-like structure collapses to a compact state in a similar way as in experiments.

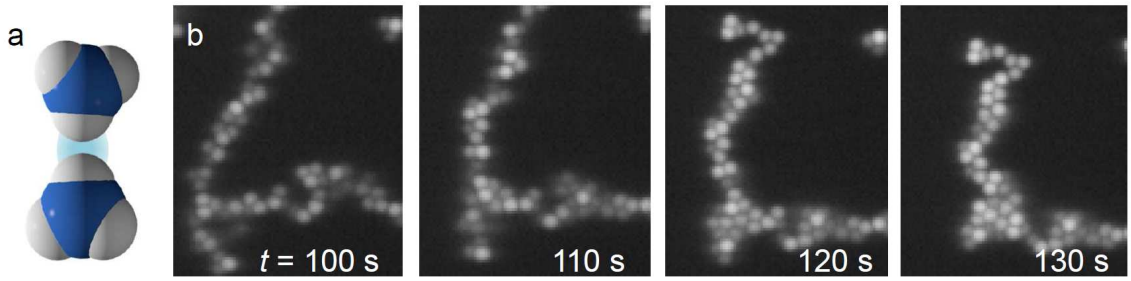

Fig. S2 Trimer particle chain collapse

(a) Patch-to-patch binding of trimer particles in 3MP-poor solvents (c_{3MP}=0.25) leading to trimer particle chains. (b) Time series showing the collapse of a trimer particle chain in 3MP-poor solvents after temperature change from ΔT=0.1 to ΔT=0.05°C. Similar to the dimer particle chains presented in the main manuscript, the trimer particles collapse into a close-packed configuration, where they can form more bonds with their neighbours.

Observation of trimer particle chain collapse

The collapse of dimer particle chains presented in the main manuscript carries over to higher-valency particles. As an example, we show the collapse of trimer particle chains in **Figure S2**. The solvent and temperature conditions are similar to those of the dimer particle collapse. As explained in the main manuscript, also the trimer particles bind with their patches in 3MP poor solvents, leading to staggered chains. When these chain-like trimer particle structures are brought to temperatures close to T_c, they collapse similar to the dimer particle chains as illustrated in Figure S2, where we show a time series after heating to $\Delta T = 0.05$°C. The trimer particle chain collapses into a more compact state, increasing the number of bonded patches. We find that this scenario occurs even for tetramer particles exhibiting four patches, demonstrating the generality of this phenomenon.

References

[1] M.T. Elsesser, A.D. Hollingsworth, K.V. Edmond, and D. J. Pine, *Langmuir* **2011**, *27***,** 917–927.

[2] V.N. Manoharan, M.T. Elsesser, D. J. Pine, *Science* **2003**, *301*, 483.

[3] J. D. Cox, *J. Chem. Soc.* **1952**, *4606*.

[4] D. Bonn, J. Otwinowski, S. Sacanna, H. Guo, G. H. Wegdam, and P. Schall, *Phys. Rev. Lett.* **2009**, *103*, 156101.

[5] M. T. Dang, A. Vila Verde, P. G. Bolhuis, P. Schall, *J. Chem Phys.* **2013**, *139*, 094903.

[6] A. Newton, A. Nguyen, D. Kraft, P. Schall and P. Bolhuis, *Soft Matter*, DOI: 10.1039/c7sm00668c.

[7] D. Frenkel and B. Smit. *Understanding molecular simulation: from algorithms to applications*, Academic Press 2001.

[8] F. Romano, C. De Michele, D. Marenduzzo, E. Sanz. *J. Chem. Phys.* **2011**, *135*, 124106.